The object of this study is the alloys of the Zr-Ti-Nb system, which better than titanium alloys meet the criterion for mechano-biocompatibility of the material for dental implants. The choice of this material is due to the fact that zirconium alloys are free of toxic elements and have a low modulus of elasticity. Under modern conditions of active implementation of additive technologies for the manufacture of metal products, the use of zirconium alloys for 3D printing is a promising area. Such technologies include electron-beam growing of products. The task solved in this work relates to the lack of technological modes for electron beam technology, specifically for zirconium alloy. A rational regime has been determined, under which samples were grown from the alloy of the Zr-Ti-Nb system with a smooth surface, uniform structure, and no internal defects. It should be especially noted that the modulus of elasticity of the material of the manufactured samples was 59.8 GPa, which is two times lower than that of the titanium alloy Ti-6Al-4V$_{ELI}$ (113.8 GPa) and is closer to the modulus of elasticity of human bone (30 GPa).

The results are explained from the point of view of physical-mechanical processes occurring in the metal during layer-by-layer surfacing under different conditions. These conditions were created by different values of technological parameters. Special feature of the results is that the formed requirements for the structure and properties of zirconium blanks were based on known dependences for titanium alloys. The findings showed that electron beam growing could become an alternative technology for manufacturing implant blanks from low-modulus zirconium alloy. The scope and conditions of practical use of the results extend to materials for implants in dentistry and, in the future, in orthopedics

Keywords: additive technologies, electron beam, energy density, layer-by-layer surfacing, dental implant, low-modulus alloy

UDC 621.791.92
DOI: 10.15587/1729-4061.2025.322118

DETERMINING TECHNOLOGICAL PARAMETERS FOR THE ADDITIVE ELECTRON-BEAM SURFACING OF BLANKS FOR MEDICAL IMPLANTS MADE OF ZR-TI-NB ALLOY

Vladyslav Matviichuk
Corresponding author
Researcher*
E-mail: vl.matviichuk@gmail.com
Vladimir Nesterenkov
Corresponding Member of the National Academy of Sciences of Ukraine, Doctor of Technical Sciences, Senior Researcher, Head of Department*
Volodymyr Efanov
PhD, Senior Researcher**
Olexandr Zavgorodny
PhD Student
Department of Integrated Technologies of Welding and Modeling of Structures
National University «Zaporizhzhia Polytechnic»
Zhukovskoho str., 64, Zaporizhzhia, Ukraine, 69063
Roman Bilyi
PhD Student**
*Department of Physical Processes, Technology and Equipment for Electron Beam and Laser Welding
E. O. Paton Electric Welding Institute of the National Academy of Sciences of Ukraine
Kazymyra Malevycha str., 11, Kyiv, Ukraine, 03150
**Department of Power Engineering
Ukrainian State University of Science and Technologies
Lazaryana str., 2, Dnipro, Ukraine, 49010

Received 31.10.2024
Received in revised form 16.12.2024
Accepted 07.01.2025
Published

How to Cite: *Matviichuk, V., Nesterenkov, V., Efanov, V., Zavgorodny, O., Bilyi, R. (2025). Determining technological parameters for the additive electron-beam surfacing of blanks for medical implants made of Zr-Ti-Nb alloy. Eastern-European Journal of Enterprise Technologies, 1 (12 (133)), 16–26. https://doi.org/10.15587/1729-4061.2025.322118*

1. Introduction

The necessary conditions for metal materials used for the production of dental and orthopedic implants are high strength and low specific weight, high corrosion resistance and biocompatibility, as well as the ability to osseointegration. Titanium alloys have proven successful in this area over many years. However, titanium alloys have a significant difference from the properties of human bone, especially in terms of the modulus of elasticity. For example, for an alloy with the Ti-6Al-4V (Grade 23) alloying system, it is E=110 GPa compared to cortical bone, E=15...30 GPa [1, 2]. All this required designing new biocompatible low-modulus alloys for medical purposes. Note that some success in solving this issue was achieved by the developed titanium β-alloy Ti-31Nb-6Zr-5Mo, which after hot deformation, aging, and subsequent heat treatment had an elastic modulus of 48 GPa [3]. Also known is the Ti-24Nb-4Zr-8Sn alloy with a Young's modulus of 49 GPa

and the Ti-24Nb-4Zr-7.9Sn alloy developed by the Chinese Academy of Sciences (E=42 GPa), which were characterized by improved biocompatibility [4, 5]. But the most popular is still the titanium alloy with the Ti-6Al-4V alloying system. Zirconium-based alloys doped with titanium and niobium are interesting and new for dentistry. The first results of studies indicate a more successful mechanical biocompatibility of this material for dental prosthetics compared to conventional titanium alloys; however, a number of unresolved issues remain. These issues are related to the technologies of production of blanks, starting from melting of ingots and ending with the creation of a finished product. Therefore, it is necessary to deal with this scientific issue for a faster introduction of zirconium alloys into the production of individualized implants. An implant that is harmoniously inscribed in the body and has material properties close to human bone is the main goal that must be achieved to improve human health in case of need for prosthetics. In this sense, zirconium alloys are the most promising material. Therefore, the results of such studies are needed in practice because they would make it possible to quickly create a high-quality replacement for lost teeth and joints by additively growing the material according to a computer model, taking into account the individual characteristics of the patient.

2. Literature review and problem statement

Research into materials for medical implants is increasingly focusing on new zirconium-based alloys that are free of chemical elements harmful to the body and have a lower modulus of elasticity (40...80 GPa) [6]. Among these alloys, low-modulus alloys of the Zr-Ti alloying system better meet the criterion for mechanical biocompatibility than titanium alloys [7, 8]. At the same time, the choice of material for implantation into the human body has controversial aspects, and some issues remain unresolved. In work [9], technological modes for obtaining alloy ingots based on the zirconium-titanium-niobium system were worked out. This paper allows us to conclude about the specificity of the technology for melting ingots of Ø110 mm zirconium alloy and the associated difficulties. In particular, the process of electron-beam melting of zirconium alloy requires special conditions – deep vacuum (up to 6×10^{-2} Pa) and an intermediate container, with cooling also in vacuum. All these factors indicate significant energy consumption. This aspect remains unresolved. Studies [6, 10] demonstrated that technological difficulties and energy consumption also accompany the manufacture of zirconium rods for the needs of dental implantology. The reason is the multi-stage deformation and thermomechanical processing to obtain a high-quality ∅6 mm rod. Under modern conditions, such an approach is not always justified since it significantly increases the price of the finished product. Therefore, it is necessary to search for new technological solutions that would avoid the indicated disadvantages. A likely option for overcoming the difficulties is to use additive manufacturing technologies. Among the additive processes, laser 3D printing and layer-by-layer electron-beam growing of articles have become the most widespread. These technologies use dispersed powders of the required alloy as the starting material. However, at this stage, difficulties may arise due to the lack of dispersed (up to 100 μm) spherical powders of zirconium alloys of the Zr-Ti-Nb system in the market, which has hindered the development of research in this area. In addition, the alloy based on the Zr-Ti-Nb system undergoes a phase transformation of the β-phase with a change in the type of crystal lattice. Rapid cooling of microvolumes of molten metal during laser printing could lead to significant structural stresses. These stresses could relax with the appearance of microcracks on the surface of the product. These features were noted in work [11]: additively manufactured alloys have a complex thermal history, which includes directional heat removal, as well as multiple melting and rapid solidification. As a rule, alloys manufactured by the additive manufacturing method also undergo repeated solid-phase transformations. These factors introduce complexities that are usually not encountered in conventional processes [12]. It could be predicted that similar trends are inherent in zirconium alloys [13]. In addition, the temperatures to which the metal is heated during laser printing could exceed 900 °C, which also makes it impossible to use protective argon (≤600 °C required) for zirconium alloy. Thus, it is necessary to choose an additive technology for growing zirconium alloy articles that is able to avoid the above-mentioned complexities. The authors of paper [14] prove that a likely option for overcoming these difficulties and implementing a controlled process of growing products in a protective environment is electron beam selective melting (EBSM). This approach has been used in the works of various researchers on the application of EBSM technology: for the nickel alloy Alloy718 [15], the titanium alloy Ti-6Al-4V [16]. That is, technological advancements concerned standard alloys, and similar studies were not conducted for zirconium alloys. Our review of the literature demonstrates that each material requires special process modes that ensure optimal microstructure and properties. Manufacturers of prostheses continue to manufacture articles from familiar, but not sufficiently compatible with the body, titanium alloys, which have already passed the certification stages and have the appropriate permits. However, for zirconium alloys, all these parameters have not been studied as thoroughly as for titanium alloys. These include technological features of thermal deformation processing, the absence of generally accepted technological regimes and recommendations that take into account the temperatures of recrystallization and phase transformations, as well as the lack of created scales of microstructures. All this gives grounds to argue that it is advisable to conduct a study aimed at optimizing technological parameters for the additive manufacturing process of articles by electron beam layer-by-layer surfacing for zirconium alloy. Thus, for the active introduction of the low-modulus Zr-Ti-Nb alloy for 3D manufacturing of medical implants using electron beam growth technology, it is necessary to solve several problems. First of all, it is necessary to establish the production of high-quality spherical powders with sizes up to 100 microns. In addition, it is necessary to devise optimal technological modes for the electron beam layer-by-layer surfacing process.

3. The aim and objectives of the study

The purpose of our research is to find rational technological modes for 3D printing of billets from zirconium alloy of the Zr-Ti-Nb system, which could make it possible to produce articles with a dense structure and improved mechanical characteristics by the additive method.

To achieve the goal, the following tasks are set:

– to investigate the properties of powders of the Zr-Ti-Nb system alloy;

– to obtain experimental samples under different technological printing parameters;

– to investigate the microstructure of the articles;

– to determine the printing modes that ensure the formation of a dispersed homogeneous microstructure with the absence of defects;

– to determine the mechanical characteristics of the experimental samples in comparison with samples from the titanium alloy of the Ti-6Al-4V system.

4. The study materials and methods

4. 1. The object and hypothesis of the study

The object of our study is the process of electron-beam 3D printing of articles from zirconium alloy powder of the Zr-Ti-Nb system.

This paper considers the features of the formation of the structure and properties of alloy blanks obtained by the method of electron-beam 3D printing. The influence of process parameters (energy density and electron beam velocity) on the formation of the structure and mechanical properties of the material was studied. The hypothesis of the study assumed that the zirconium alloy of the Zr-Ti-Nb system, similarly to titanium alloys, significantly depends on the structural state, which for 3D printing depends on the specific energy of the electron beam. It was also assumed that these alloys are sensitive to the presence of any defects that act as stress concentrators. As is known, any concentrator could become a place of origin of destructive processes. For titanium alloys, it is known that the dispersed globular structure has higher strength indicators and sufficient plasticity while a coarse-grained, lamellar structure is undesirable because it produces low mechanical properties. These relationships were also assumed for the zirconium alloy under study.

Therefore, the process parameters must be selected according to such indicators as the absence of defects such as porosity and other discontinuities while maintaining the maximum dispersed microstructure. It is assumed that excessive specific energy received by the volume of the material being fused leads to the formation of a coarse-grained structure of the formed material, characteristic of the overheated state. Accordingly, this would lead to a decrease in the mechanical characteristics of the resulting workpiece. Therefore, the power of the electron beam, the scanning speed, the scan line offset step, and the thickness of the powder layer could be used as tools for influencing the processes of material formation. Variating these parameters leads to a change in the values of specific energy per unit volume of the powder being fused and, accordingly, changes the kinetics of melting and subsequent crystallization. Therefore, to select rational parameters for the 3D printing mode of the Zr-Ti-Nb alloy system, it is necessary to conduct a comprehensive study on the influence of features in the formation of the macro- and microstructure on the set of mechanical characteristics of the alloy.

4. 2. Materials and equipment

For the research, we used ZTN-4 grade powder of Zr-Ti-Nb alloy, which was produced by rotary plasma spraying of a bar billet using the equipment and technology of "Multiflex" LTD (Ukraine) [17]. The powder particles had an average diameter of 40 to 160 microns, were of regular spherical shape (Fig. 1). The chemical composition of the zirconium alloy powder was determined by the spectral method using the "Expert 3" device (given in Table 1). The essence of the method is based on determining the intensities of the excited spectrum from each chemical element, which is directly proportional to its mass fraction in the alloy.

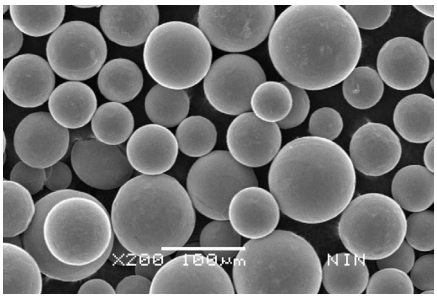

Fig. 1. General view of ZTN-4 powder from Zr-Ti-Nb alloy

Table 1

Chemical composition of ZTN-4 grade powder from Zr-Ti-Nb alloy, % (wt.)

ID	Ti	Nb	Zr
Actual powder composition	20.0	19.7	59.9
Permissible range for Zr-Ti-Nb alloy [17]	15–30	15–30	40–65

In our earlier work on the additive growing of titanium blanks, we have reasonably chosen electron-beam additive technology, described the equipment available in Ukraine, and reported the results of its modernization. Equipment for electron-beam 3D printing (Fig. 2) was designed at the E. O. Paton Electric Welding Institute of the National Academy of Sciences of Ukraine [18, 19].

The sequence of stages of additive electron-beam production was as follows [20]: first, a 3D model of the object was built. The next stage required transferring the file to the additive equipment. Then the 3D printer constructed the articles layer by layer. After building and cooling, the assembly was removed from the equipment. Then, cleaning, polishing, and surface finishing of the parts were performed.

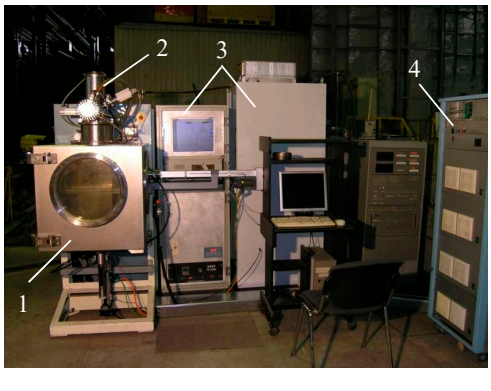

Fig. 2. Experimental additive equipment:
1 – vacuum chamber; 2 – electron beam gun;
3 – control cabinets; 4 – high-voltage source [19]

The surfacing processed in a vacuum chamber 1 (Fig. 2). The thickness of one deposited layer was approximately 100 μm. The accelerating voltage of the electron beam gun 2 was 60 kV. The preliminary heating of the powder layer to a temperature of 680 °C was carried out by a raster

beam with a power of 1800 W. The working pressure during surfacing was 10^{-2} Pa.

A description of the equipment, technological parameters, and the surfacing process is given in [21]. To determine the metal structures, 25 samples were printed with a size of 25×25 mm, a height of 5 mm, of which 2 mm were technological supports.

To study the mechanical characteristics, experimental samples were printed: 15×80×5 mm and 12×55×14.5 mm, the height of the technological supports of the experimental samples was 2.5 mm (Fig. 3).

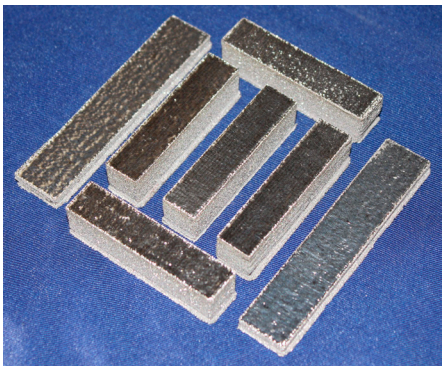

Fig. 3. Printed sample blanks for mechanical testing

Samples for uniaxial tensile and impact bending tests, as well as for determining the elastic modulus, were made from the blanks.

The printing mode of the samples for determining the mechanical properties was selected based on the results of investigating the macro- and microstructure of the samples for metallographic studies. For comparing the properties, samples from the Ti-6Al-4V alloy were also selected, which were also made using the additive electron beam surfacing technology. The implementation of this technology is described in [22].

4. 3. Research methods

The bulk density of the powder was determined using the funnel method according to ISO 4490-78.

The microstructure of the samples was studied by sequential grinding using abrasives of different grain sizes (from No. 40 to micron paper (M20). At the final stage, the micro sections were polished on a coat cloth moistened with a suspension of "DiaDuo" (manufacturer "STRUERS") based on diamond particles with a fraction of 3 microns. For metallographic analysis, the zirconium alloy powder was poured into electrically conductive Bakelite and polished using diamond suspensions. The sections were etched in the reagent: HF – 10 ml, HNO_3 – 25 ml, glycerin – 65 ml. The microstructural analysis was performed using an inverted reflected light microscope "Observer.D1m" (Carl Zeiss). The macrostructure was studied using a stereomicroscope "Stemi 2000-C" ("Karl Zeiss"). X-ray spectral microanalysis (XSMA) was performed using a detector "Bruker" and software "Esprit" on scanning electron microscope "Hitachi SU3900" with an accelerating voltage of 15 kV.

To study mechanical characteristics, we used blanks measuring 12×12×55 mm, which were made of Zr-Ti-Nb alloy by electron beam surfacing [29], as well as samples from medical titanium alloy Ti-6Al-4VELI [23]. Uniaxial tensile tests were performed on an INSTRON-8862 tensile testing machine at a gripper movement speed of 15 mm/min. In accordance with the ISO 6892-1:2019 standard, proportional samples with a diameter of 5 mm with a cylindrical working part were manufactured. Impact bending tests were performed on an IMP – 460J ("INSTRON") pendulum impactor with a nominal potential energy of the pendulum of 460 J. The samples were manufactured with a U-shaped concentrator. For the tests, blanks were used, which were subsequently milled and polished (Fig. 4). U-shaped cuts on the samples were made on a milling machine. A typical appearance of the sample after testing by the pulse excitation method is shown in Fig. 5. The samples were made from flat blanks with dimensions of 15×3×80 mm.

Fig. 4. Impact bending test samples made from electron beam printed blanks

Fig. 5. General view of the sample after testing to determine the modulus of elasticity

The elastic modulus (Young's modulus) was determined by the pulse excitation method [24] on the RFDA Professional System 24 (Belgium). The method was used to obtain the most accurate result due to the fact that prosthetic materials are low-modulus. The essence of the method was that mechanical vibrations in flat-shaped test samples were excited by a blow from a striker. The Young's modulus was determined by measuring resonant frequencies. The resulting signal was calculated by fast Fourier transform. Specialized software determined the resonant frequency with high accuracy for calculating elastic properties based on the Euler-Bernoulli theory.

5. Results of research on experimental samples

5. 1. Determining the properties of powder materials

The fractional composition of the resulting metal powders of the Zr-Ti-Nb alloy is given in Table 2, in which D_{10}, D_{50} and D_{90} represent a percentage of the total volume of the powder.

For the additive process of electron beam manufacturing of samples from the studied zirconium alloy, a powder was used that corresponded to the average diameter of the granules D_{50}=60...85 μm.

The structure of the powder particles consisted of a combination of α- and β-phases. Annealing mode: heating to a temperature of 440 °C, aging for 1.5 hours in the furnace, and

slow cooling in air [17]. During the microstructural analysis of the micro sections, it was found that the used powder met the requirements for additive technologies: the particle structure is homogeneous and dispersed, internal porosity in the powder particles was not detected (Fig. 6). The distribution of chemical elements in the powder particles is homogeneous, which was confirmed by the results of micro-X-ray spectral research in the form of element distribution maps (Fig. 7) [25].

Table 2

Fractional composition of Zr-Ti-Nb alloy powders

Fraction		Bulk density, g/cm^3	Weight, g
+200		4.20	900
+180		4.19	128
–140+125		4.00	2654
–90+56		3.97	1589
–56+40		3.97	95
–40		3.96	261
Distribution by fractions for powder (–90+56), μm	D_{10}	54…58	
	D_{50}	60…85	
	D_{90}	90…110	

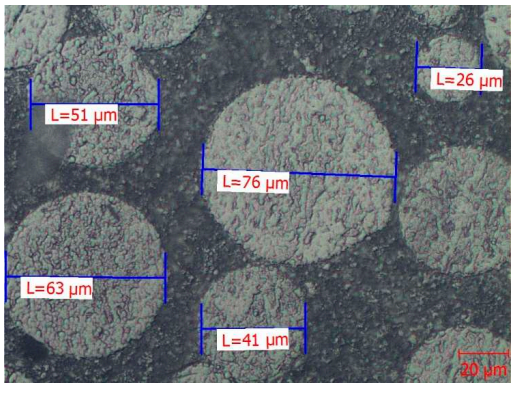

Fig. 6. Microstructure of Zr-Ti-Nb alloy powder particles (particle measurements were performed by microscope software), ×500

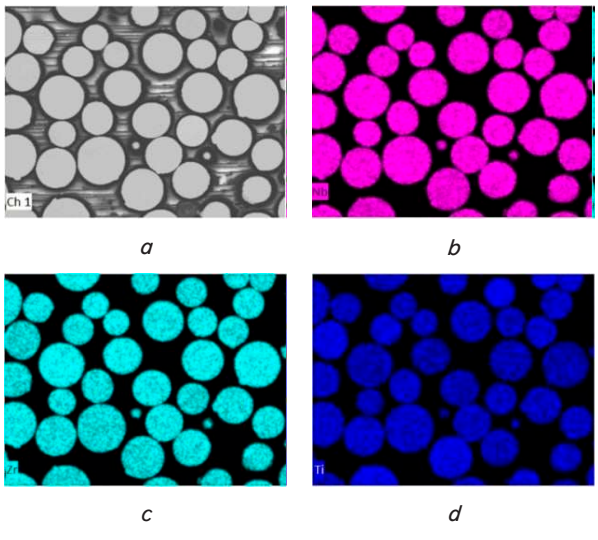

Fig. 7. Distribution maps of chemical elements of powder particles from the Zr-Ti-Nb alloy obtained by X-ray spectral microanalysis: *a* — general view of powder particles on an electron microscope; *b* — niobium; *c* — zirconium; *d* — titanium

From the data illustrated in Fig. 6, 7, it could be concluded that the powder used for electron beam printing of experimental samples met the quality criteria for powders in additive technologies.

5. 2. Production of experimental samples under different technological printing parameters

Samples for studying the metal structure were made from zirconium alloy powder of the Zr-Ti-Nb system. Five electron beam velocity regimes were investigated: 250 mm/s, 500 mm/s, 750 mm/s, 1000 mm/s, 1500 mm/s. The thickness of the metal powder layer was 100 μm. The scanning strategy was selected as bidirectional, serpentine. The beam trajectory displacement step was 0.2 mm. In this case, the scanning direction was rotated by 90° for each layer. The electron beam energy density was changed from 30 to 70 J/mm^3 for each beam velocity value. A description of the surfacing technological parameters and their relationship is given in [21].

Sequential electron beam growing of samples was performed under modes in which two parameters were changed: scanning speed (mm/s) and electron beam energy density (J/mm^3). The scanning speed was changed in the range from 250 mm/s to 1500 mm/s. The influence of electron beam energy density was studied in the range from 30 to 70 J/mm^3. The parameters of the electron beam manufacturing process include speed, electron beam power, powder layer thickness, and beam trajectory offset step. The integrated parameter that combined all process parameters was the beam energy density. This parameter was used to describe the influence of these characteristics on the structure and material properties of the samples. The condition of the sample surface was assessed visually. The initial inspection of the surfaces allowed us to divide the samples into three groups: rough, smooth, and bumpy. The correspondence of the printing technological parameters and the surface condition of the samples is shown in Fig. 8.

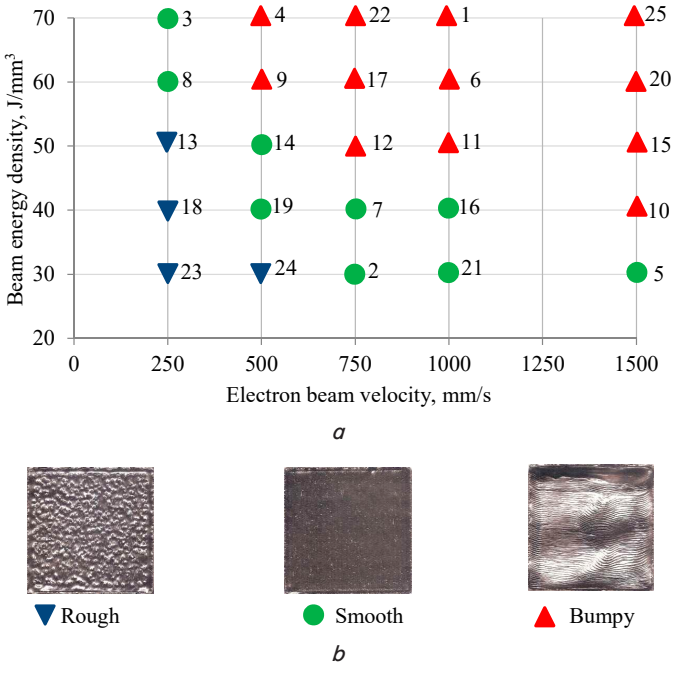

Fig. 8. Influence of technological printing parameters on the surface morphology of samples: *a* — grouping of samples by type of surface morphology; *b* — surface morphology of samples, which is the basis for grouping

Visual inspection of the samples showed that on the surface of individual samples (for example, No. 15, No. 20, No. 25) there was a conical protrusion in the central part (Fig. 9, *a–c*).

On samples without conical protrusions, but with high roughness (for example, No. 18, No. 23, No. 24 – Fig. 9, *d–f*), the formation of such a surface occurred under conditions of low electron beam energy density and its slow movement.

Other samples with a higher electron beam energy density (No. 3, No. 8) or with an increase in electron beam velocity (for example, No. 7, No. 14, No. 19) had a more even and smooth surface (Fig. 9, *g–i*).

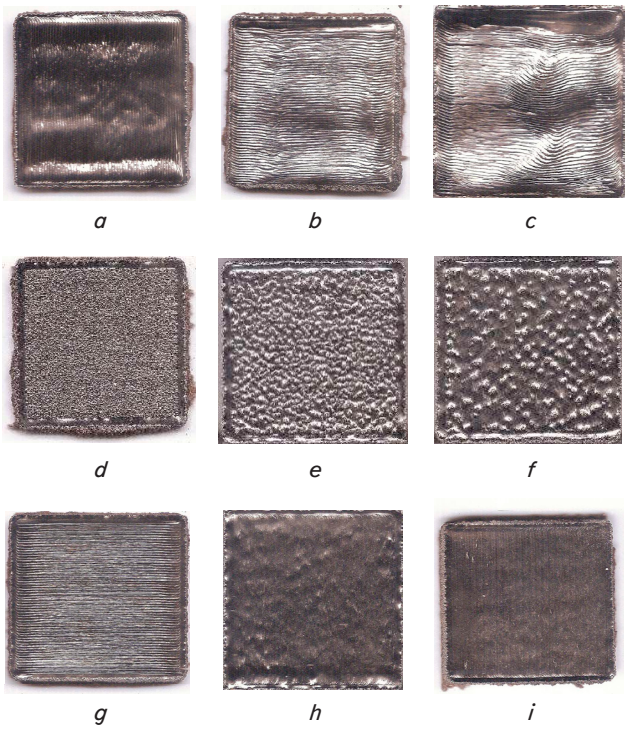

Fig. 9. External condition of the surface of samples formed using different technological modes of electron beam surfacing: *a—c* — with local protrusion; *d—f* — rough; *g—i* — lines of surfaced layers are smoothed

One can see from Fig. 9 that high surface quality (morphology type – smooth) was obtained using different combinations of technological parameters. Such surface morphology was formed at energy density values ranging from 30 J/mm^3 to 70 J/mm^3 and beam velocity from 250 mm/s to 1500 mm/s.

It should be noted that the surface of sample No. 19 was characterized by the smoothest relief, there were no defects on the surface of the given sample (Fig. 10).

Fig. 10. The external condition of the surface of sample No. 19, formed using the electron beam surfacing technological mode: beam energy density 40 J/mm^3 and its movement speed 500 mm/s

Therefore, from the point of view of surface formation, the printing mode of sample No. 19 with technological parameters such as beam energy density of 40 J/mm^3, speed of its movement of 500 mm/s was considered rational.

5. 3. Study of the microstructure of samples

In addition to the surface condition, an important characteristic of the material grown using additive technology is its microstructural condition and the absence of microdefects (pores, sinks, etc.) over the entire cross-section.

So, metallographic study of the samples was carried out by comparing the metal structure for the presence of defects in the form of any discontinuities, as well as from the point of view of the formed microstructure (grain size, type of structure).

Microanalysis of cross-sections made it possible to establish that in the samples obtained with the lowest energy density and with a low electron beam velocity (No. 18, No. 23, No. 24), non-fusion was detected at the interface of the layers and in the zone of technological supports (Fig. 11).

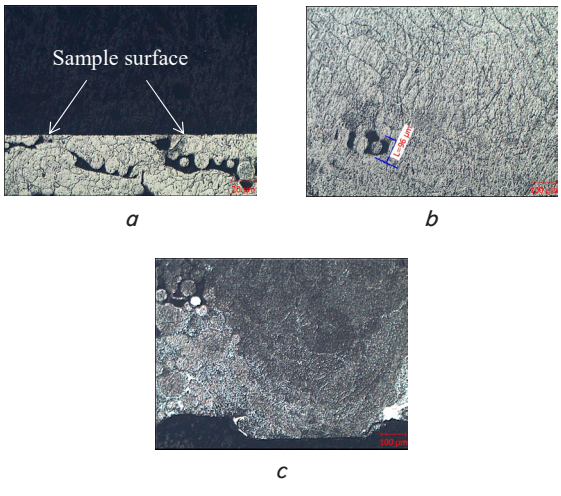

Fig. 11. Discontinuities in the microstructure of samples (cross micro sections): *a* — defects protruding onto the surface of the sample; *b* — internal pores; *c* — non-fusion of powder particles

When analyzing the micrographs, it was found that discontinuities partially protrude onto the surface of the samples (Fig. 11, *a*), which caused their high roughness.

In samples grown with a high electron beam energy density (60...70 J/mm^3), round and elliptical micropores from ∅30 to ∅60 μm were found (Fig. 12, *a*, *b*).

In samples grown with a lower energy density and a high electron beam velocity, micropores were also found. It should be noted that their size was up to ∅15 μm and was single in nature, the pores did not protrude onto the surface of the sample (Fig. 12, *c*, *d*).

At the minimum electron beam speed (250 mm/s) and energy density from 20 J/mm^3 to 50 J/mm^3, the material structure of the experimental samples consisted of columnar dendrites with dimensions of ~50...130 μm (Fig. 13, *a*).

When the energy density increased to 40...50 J/mm^3 and the electron beam speed was 500–750 mm/s, crystallization proceeded faster due to the greater temperature difference between the layers. At the same time, the columnar grains became shorter or approached equiaxed grains with a diameter of 40...50 μm (Fig. 13, *b*, *c*). When the beam speed

increased to 1000...1500 mm/s, grain enlargement and thickening of the intergranular boundaries occurred (Fig. 13, *d*). Such a coarse-grained microstructure is characteristic of a heating temperature above the polymorphic transformation temperature, the grain size being 100...130 μm. The optimal microstructure was taken to be an equiaxed type with a grain size of about 40 μm, which was achieved with the following process parameters: 40...50 J/mm^3 and an electron beam velocity of 500...750 mm/s (Fig. 13, *c*), which corresponds to the printing modes of samples No. 7, 14, 19.

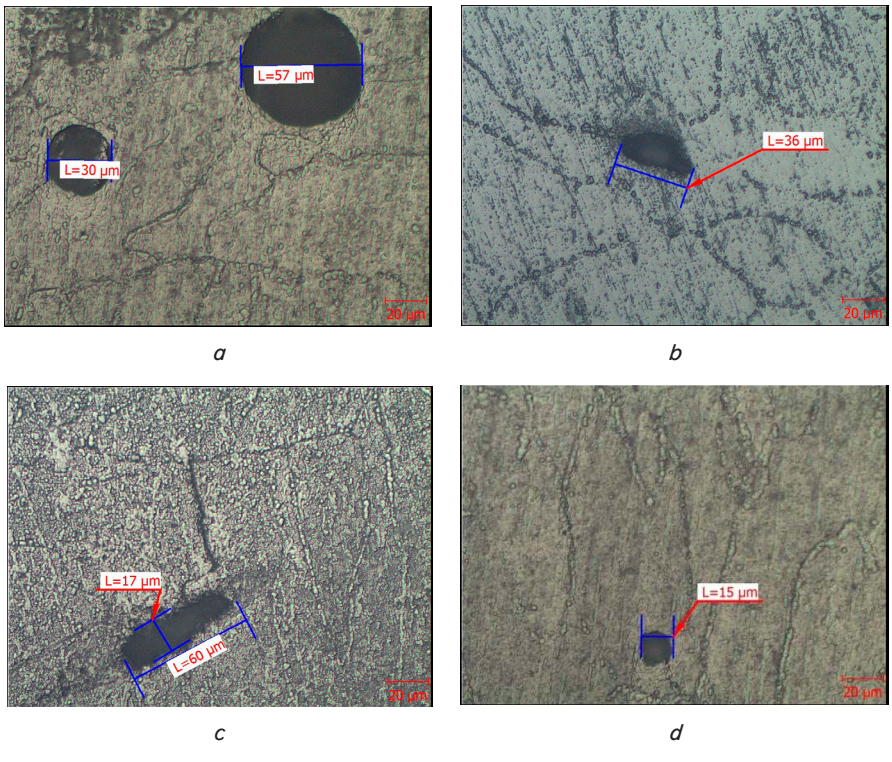

a *b* *c* *d*

Fig. 12. Types of micropores in the material of samples grown by electron beam surfacing (×500): *a* – rounded pores ∅30...57 μm; *b* – elliptical pore with a length of 36 μm; *c* – large pore with a crack; *d* – internal pore ∅15 μm (sample No. 19)

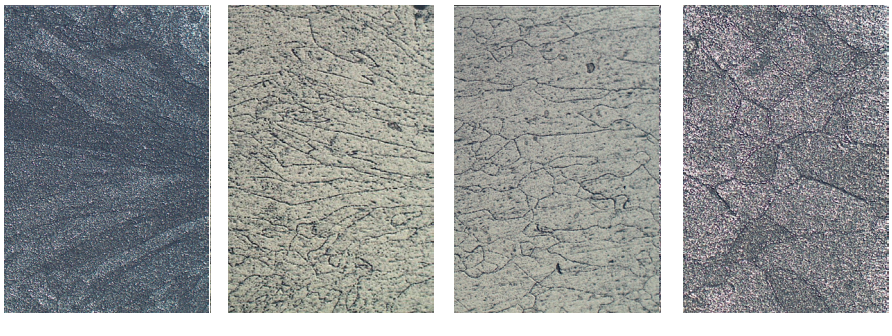

a *a* *a* *a*

Fig. 13. Typical microstructures of samples from the Zr-Ti-Nb alloy (×100) grown by electron beam surfacing under different modes: *a* – 250 mm/s, 30 J/mm^3; *b* – 500 mm/s, 30 J/mm^3; *c* – 500 mm/s, 40 J/mm^3 (sample No. 19); *d* – 1500 mm/s, 70 J/mm^3

The microstructures shown in Fig. 13 clearly demonstrate the influence of thermal energy and electron beam velocity on the structure formation of the zirconium alloy Zr-Ti-Nb; the alloy is structurally sensitive and requires the construction of scales for permissible and impermissible structures. The results obtained could form the basis of such a scale.

5. 4. Determining printing modes that enable the formation of the best structural state

When determining the printing modes that provided the best structural characteristics, it was found that sample No. 19 had a high surface quality (Fig. 10). At the same time, the metal was characterized by complete fusion in its cross section, and the presence of a single micropore with a diameter of up to 15 μm could be caused by shrinkage processes (Fig. 12, *d*). The microstructure of the specified sample belonged to the equiaxed type with a grain size of about 40 μm (Fig. 13, *c*).

From Fig. 8 it follows that the printing of sample No. 19 was carried out with a beam speed of 500 mm/s and an energy of 40 J/mm^3. The specified mode provided a dispersed microstructure and surfacing with minimal influence of discontinuities, contributed to the formation of the smallest grain size among samples with high surface quality. Therefore, this mode was chosen for the manufacture of samples for mechanical testing.

5. 5. Determining the mechanical characteristics of test samples

The summarized values of mechanical characteristics of zirconium and titanium alloys are given in Table 3.

The results of mechanical tests of zirconium alloy samples showed that the resulting material has a modulus of elasticity twice as low as that of Ti-6Al-4VELI alloy, and an impact strength approximately at the level of titanium alloy. Strength and ductility characteristics are somewhat lower than titanium alloy.

It is also important to compare the properties of samples of zirconium and titanium alloys grown using electron beam printing technology. Table 3 gives the mechanical properties of samples of titanium alloy Ti-6Al-4V, manufactured by electron beam surfacing: their strength characteristics significantly exceed those of zirconium alloy and the properties of a standard bar of this alloy for dental purposes.

A typical form of the tensile diagrams of the studied samples of the Zr-Ti-Nb alloy is shown in Fig. 14. The tensile curve had characteristic sections: proportionality (up to stresses of about 620 MPa), a material yield plateau of 700 MPa, and a tensile strength of about 720 MPa (Fig. 14).

The fracture surfaces of the samples under the action of impact loading were characterized by a fine-crystalline structure (Fig. 15, *a*). It should be noted that on the fracture surface layers of deposited metal were found in the form of thin stripes, which at different angles of view had a dark or light shade. It is seen that the structure of the metal is dense,

without defects (Fig. 15, *b*). As a result of our study using an electron microscope (Fig. 16) it was established that the nature of the fracture of the samples was viscous, had a pitted microrelief.

Table 3

Comparison of mechanical properties of samples grown using additive electron beam printing technology from zirconium alloy Zr-Ti-Nb and titanium alloy Ti-6Al-4V

Material	σ_b, MPa	$\sigma_{0.2}$, MPa	E, GPa	δ, %	KCU, J/cm^2
Zr-Ti-Nb (electron beam growing)	726	701	59.83*	5.2	4.1
Ti-6Al-4V$_{ELI}$ [6] standard rod	860	790	113.8	15	3.2**
Ti-6Al-4V [26] (electron beam growing)	1032	973	–	12	–

*Note: * – determined by the pulse excitation method; ** – the sample was cut from a standard rod ∅12 mm of Ti-6Al-4V alloy.*

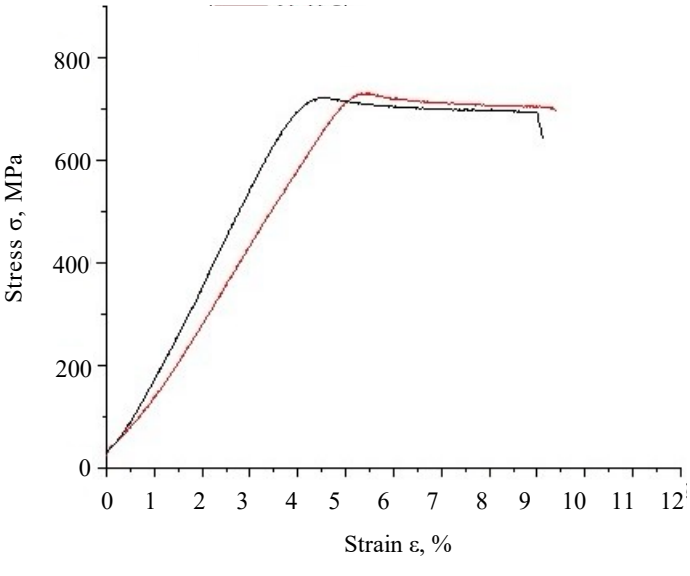

Fig. 14. Tensile diagram of tested samples of Zr-Ti-Nb alloy grown by electron beam technology (different color corresponds to different samples)

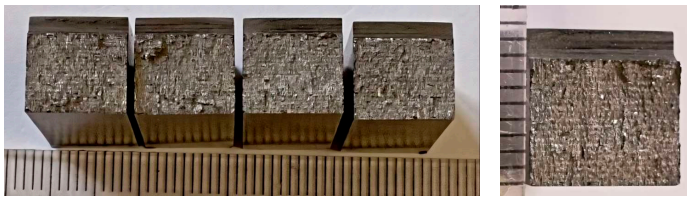

a *b*

Fig. 15. Macrostructure of fracture surfaces of samples after impact bending tests (view at different magnifications): *a* – ×3; *b* – ×12.5

Fig. 16 demonstrates that the interface of the deposited layers is not detected at electron microscope magnifications; the grown material is monolithic and homogeneous.

Therefore, the electron beam growing mode with a beam energy density of 40 J/mm^3 and a movement speed of 500 mm/s could be recommended for the manufacture of dental implants from zirconium alloy Zr-Ti-Nb.

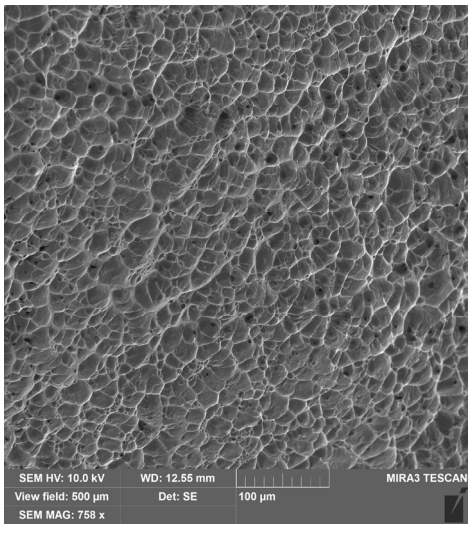

Fig. 16. Microrelief of the fracture surface of the sample after mechanical testing, ×800

6. Discussion of results based on the research into the structure and properties of Zr-Ti-Nb alloy billets obtained by the additive method

The quality of articles manufactured using additive technologies primarily depends on the starting material – powder. As is known, the main requirements for the quality of additive powder are the following:

– sphericity;

– absence of satellite particles on the surface;

– the surface of the granules must be smooth and unoxidized;

– the composition of the powder does not allow non-metallic particles or particles of another metal;

– the chemical composition and microstructure of the powder particles must be homogeneous, without micropores and non-metallic inclusions;

– the size of the powder particles must not exceed 100 microns.

The size and shape restrictions are related to the technological properties of the powder – smooth spherical particles have better flowability and bulk density. In turn, the strict requirements for the quality of the metal of the powder particles are related to the fact that these characteristics could be inherited by articles printed from this powder. The centrifugal plasma spraying mode is combined, where the metal of each powder particle undergoes quenching during cooling, and the subsequent separate heat treatment. This allowed creating a special phase and structural state of the powder granules – a structure of dispersed micro grains (Fig. 6). When forming such a microstructure in the powder particles, the chemical elements are evenly distributed, there are no microleakages, which was confirmed by the results of X-ray spectral microanalysis (Fig. 7).

Therefore, our studies of zirconium alloy powder with the Zr-Ti-Nb alloying system have made it possible to establish that the powder used for electron beam printing of experimental samples met the quality criteria for powders in additive technologies.

As shown in studies on various alloys [1, 4], the energy density of the electron beam and the speed of its movement affect the state of the resulting surface. Thus, in some cases

it is smoother, in others it is rougher, bumpy, or with conical protrusions, which is unacceptable for the finished product and requires additional processing operations. Therefore, the criterion for surface quality was chosen as a flat and smooth surface with the lowest roughness. The roughness of the surface varied depending on the amount of specific energy introduced into the material during the printing process. With excessive melting intensity, a conical protrusion was formed on the surface of individual samples (No. 15, No. 20, No. 25) in the central part. This could be explained by the high concentration of beam energy during their creation (Fig. 8, 9, *a–c*). The combination of these factors (high energy density and maximum beam movement speed) caused the accumulation of thermal energy and uneven temperature distribution in the body of the sample. At the same time, on some samples without conical protrusions (Fig. 9, *d–f*) a surface with high roughness was formed (for example, samples No. 18, No. 23, No. 24). Such a surface was created under conditions of low energy density of the electron beam and its slow movement. Therefore, the manufacture of samples according to technological modes No. 18, No. 23, No. 24 led to uneven melting of the metal throughout the thickness of the layers. As a result, crystallization defects (micropores, non-fusion of powder particles, etc.) were detected in the cross-section of the samples, which also had access to the surface and thereby increased its roughness. Therefore, the selected quality criteria were met by, for example, samples No. 16, 18, 24 (Fig. 9, *g*, *i*) and sample No. 19 (Fig. 10). The specified samples were manufactured under conditions of moderate intensity of specific energy of the electron beam and sufficient speed of its movement.

In addition to the surface condition, an important characteristic of the material grown using additive technology is its microstructural condition and the absence of microdefects (pores, sinks, etc.) over the entire cross-section. The presence of microdefects in the studied samples, shown in Fig. 11, 12, is associated with insufficient temperature for fusion of powder particles and directly layers due to the low energy density of the process. In samples grown with a high energy density of the electron beam (60…70 J/mm^3), round and elliptical micropores ∅30–60 μm were found, examples of which are shown in Fig. 12. This could be explained by shrinkage processes under conditions of maximum rapid beam movement and rapid crystallization of the deposited layers. Micropores could become stress concentrators and the site of crack initiation. Therefore, pores are unacceptable for articles of critical purpose, such as implants.

The materials science approach to solving problems of various metallic materials implies that the required level of mechanical properties is provided by a certain chemical composition and its microstructure. When working with one alloy, the chemical composition is a constant parameter. In turn, the microstructure of samples grown under different conditions changed. To assess the microstructure, a dispersed equiaxed microstructure was chosen as the standard, which is characteristic of titanium alloys with high strength characteristics and resistance to fatigue fractures – regulated for highly loaded aviation parts.

Considering the closeness of the atomic radii of zirconium and titanium, as well as similar physical and mechanical properties of these elements, it was assumed that the zirconium alloy Zr-Nb-Ti would have similar dependences. The microstructure of Zr-Ti-Nb alloys is similar to titanium alloys and is formed according to the same principles. Namely, during casting, a dendritic structure is formed, the size of the dendrite cells depends on the heat removal rate, which depends on the energy of the electron beam, the scanning speed, and the thickness of the deposited layer. During deformation, the coarse microstructure is crushed, and various stages of recrystallization occur, the starting temperature of which depends on the degree of deformation.

The best combination of strength and ductility is usually provided by a fine-grained equiaxed microstructure, higher fatigue strength is provided by alloys with a lamellar misoriented microstructure. Large lamellar grains and grains with a thick rim from other phases usually have alloys with low strength and ductility. Therefore, the criteria for evaluating the microstructure were:

– type of structure (dendritic, equiaxed, lamellar);

– grain size and thickness of intergranular boundaries.

A satisfactory microstructure of the studied zirconium alloy was considered to be an equiaxed type structure with a grain size from 15 μm to 40 μm, with thin intergranular boundaries.

By changing the technological modes of electron beam surfacing, it is possible to influence the process of structure formation, therefore, it is possible to obtain the required microstructure and material properties of the experimental samples from the Zr-Ti-Nb alloy.

Thus, at the minimum electron beam velocity (250 mm/s), the material structure of the experimental samples consisted of columnar dendrites with dimensions of ~50…130 μm, elongated in the direction of heat removal (shown in Fig. 13, *a*). This was probably due to the rather slow heat removal between the deposited layers and the low temperature gradient. In samples manufactured with a beam energy density within 30 J/mm^3, the microstructure consisted of more compact grains, somewhat elongated in the direction of heat removal. With an increase in the electron beam energy density to 40 J/mm^3, the grains in the microstructure of the samples approached the equiaxed form, their size was 20…40 μm. Such changes in the microstructure are probably associated with a more uniform distribution of thermal energy. Such a distribution allows the metal grains to crystallize quickly, and the grains do not have time to grow. Significant grain growth was observed in the microstructure of samples manufactured at a beam energy of 70 J/mm^3. In addition to the grain size, the thickness of the grain boundaries has a significant impact on the properties of the alloy. Thickened grain boundaries due to the separation of the second phase in the form of a mesh negatively affect the strength and ductility. Comparing the structure of the studied samples of the Zr-Nb-Ti alloy, it could be concluded that thinner and broken grain boundaries were observed in sample No. 19. Thus, according to the results of metallographic research, the most rational structure and surface condition of the samples were formed with the electron beam surfacing mode: 500 mm/s, 40 J/mm^3. This mode was chosen for growing prismatic blanks for samples for mechanical tests.

The results of mechanical tests of zirconium alloy samples showed that the obtained material had a modulus of elasticity 2 times lower than that of the Ti-6Al-4VELI alloy, and an impact strength approximately at the level of the titanium alloy. The strength characteristics and plasticity are somewhat lower than those of the titanium alloy. It is also important to compare the properties of the studied zirconium samples with titanium samples grown using the same electron beam printing technology. Table 3 gives the mechanical properties of samples of the titanium alloy Ti-6Al-4V, manufactured by electron beam surfacing, for comparison. The data presented show that the strength characteristics of the titanium alloy significantly exceed the zirconium alloy and the properties of a standard bar of this alloy for dental purposes. This could be explained from the point of view of microstructural differences between a standard deformed bar in the annealed state and a sample of the Ti-6Al-4V alloy grown by electron beam. In small diame-

ter rods, as a rule, the microstructure belongs to the equiaxed type with the dimensions of the α/β-phases within 20…40 μm. At the same time, as a result of electron beam surfacing, a fine-plate morphology of the α/β-phases or a mixture of the stable α-phase and α′-phase of the martensitic type could be formed. The martensitic microstructure in this case is formed as a result of rapid cooling of thin layers of the deposited metal.

It should be noted that ultra-high strength does not always satisfy the operating conditions of implants and could significantly exceed the properties of human bone. Therefore, doctors are more often guided not by strength but by the modulus of elasticity of the material and a sufficient margin of plasticity and toughness, biocompatibility of the alloy, etc. [10]. In this sense, the mechanical properties of the zirconium alloy Zr-Ti-Nb samples grown by electron beam technology could become a competitive alternative to titanium alloys. The presence of a pitted microrelief on the fracture surface of the samples after mechanical tests characterizes the ability of the Zr-Ti-Nb alloy to plastic deformation. This, along with the low modulus of elasticity, makes the zirconium alloy more suitable than titanium for use in the manufacture of implants.

Thus, as a result of electron beam growth, samples of an alloy based on Zr-Nb-Ti with a high-quality surface, without internal defects and with a satisfactory level of mechanical properties were obtained. At the same time, the elastic modulus of the obtained material is closer to the elasticity of human bone than the titanium alloy Ti-6Al-4V.

For the manufacture of dental implants from zirconium alloy Zr-Ti-Nb, a rational mode of electron beam growth was chosen (electron beam movement speed 500 mm/s, beam energy density 40 J/mm^3).

Our research results have limitations. These are, first of all, the small sizes of the obtained workpieces. Additional studies are necessary for the manufacture of larger workpieces by electron beam layer-by-layer surfacing, which is required, for example, in orthopedics. Secondly, there is a question of lower plasticity compared to the titanium alloy Ti-6Al-4VELI. It is necessary to find out how much the dental implant requires a reserve of plasticity at the level of a titanium alloy. This issue could be resolved by modeling the implant load, for example, using the finite element method. The research also did not determine the effect of heat treatment on the structure and material properties of the resulting blanks, which could be attributed to the shortcoming of this work. This provides a basis for further research on low-modulus zirconium alloys.

7. Conclusions

1. Our studies allowed us to establish that the powder from the Zr-Ti-Nb alloy system, used for electron beam printing of experimental samples, met the quality criteria for powders in additive technologies. The main ones are the average size of the powder particles, which was 60…85 microns, a homogeneous structure, and chemical composition.

2. Experimental samples were manufactured using 25 electron beam surfacing modes. As a result, the samples were grouped into three types according to the surface condition: rough, smooth, bumpy. It was established that the bumpiness and rough surface are due to the presence of crystallization defects – micropores, discontinuities, the size of which decreased (from 60 microns to 15 microns) with a decrease in the beam energy density. No defects were found in the material of individual samples, their surface was characterized as smooth.

3. The microstructures of the obtained samples from the Zr-Ti-Nb alloy system differed in grain size and shape. The dispersion and morphology of the grains changed depending on the specific energy transferred by the electron beam. At its low values (30 J/mm^3), the microstructure of the samples was characterized by elongated grains oriented in the direction of heat removal. At the same time, microdefects (pores, non-fusion) were detected in the structure. An increase in energy to 40 J/mm^3 contributed to the formation of a dense metal structure with equiaxed grains of 40…50 μm. Excessive melting intensity (70 J/mm^3) caused grain growth (≥100 μm) and the formation of pores.

4. Electron-beam 3D printing under the defined mode (beam speed 500 mm/s, energy density 40 J/mm^3) made it possible to form a dispersed microstructure and a surface without defects in the sample material. The results of our research showed that electron-beam growth makes it possible to produce blanks for dental implants of high quality from spherical powders of the Zr-Ti-Nb alloy.

5. The mechanical properties of the material of the samples grown using electron-beam printing technology from the zirconium alloy Zr-Ti-Nb are somewhat lower in terms of strength and plasticity than the titanium alloy Ti-6Al-4V. At the same time, the value of the elastic modulus of zirconium samples is up to 2 times lower than that of titanium and is closer to the properties of human bone.

Conflicts of interest

The authors declare that they have no conflicts of interest in relation to the current study, including financial, personal, authorship, or any other, that could affect the study, as well as the results reported in this paper.

Funding

The work was funded within the framework of the National Academy of Sciences of Ukraine target research program on the topic “Devising technologies for obtaining the state-of-the-art titanium alloys by electron beam melting methods and articles from them by rolling and 3D printing methods for defense and medical needs” (State registration number 0123U100870).

Data availability

The data will be provided upon reasonable request.

Use of artificial intelligence

The authors confirm that they did not use artificial intelligence technologies when creating the current work.

Acknowledgments

The authors are grateful to the State Firm “Engineering Center of Electron Beam Welding” E. O. Paton Electric Welding Institute NAS of Ukraine for technical support in conducting the research.

References

1. Fellah, M., Labaïz, M., Assala, O., Dekhil, L., Taleb, A., Rezag, H., Iost, A. (2014). Tribological behavior of Ti-6Al-4V and Ti-6Al-7Nb Alloys for Total Hip Prosthesis. Advances in Tribology, 2014, 1–13. https://doi.org/10.1155/2014/451387
2. Elias, C. N., Lima, J. H. C., Valiev, R., Meyers, M. A. (2008). Biomedical applications of titanium and its alloys. JOM, 60 (3), 46–49. https://doi.org/10.1007/s11837-008-0031-1
3. Liang, S. X., Feng, X. J., Yin, L. X., Liu, X. Y., Ma, M. Z., Liu, R. P. (2016). Development of a new β Ti alloy with low modulus and favorable plasticity for implant material. Materials Science and Engineering: C, 61, 338–343. https://doi.org/10.1016/j.msec.2015.12.076
4. Nune, K. C., Misra, R. D. K., Li, S. J., Hao, Y. L., Yang, R. (2017). Osteoblast cellular activity on low elastic modulus Ti–24Nb–4Zr–8Sn alloy. Dental Materials, 33 (2), 152–165. https://doi.org/10.1016/j.dental.2016.11.005
5. Shi, L., Shi, L., Wang, L., Duan, Y., Lei, W., Wang, Z. et al. (2013). The Improved Biological Performance of a Novel Low Elastic Modulus Implant. PLoS ONE, 8 (2), e55015. https://doi.org/10.1371/journal.pone.0055015
6. Mishchenko, O., Ovchynnykov, O., Kapustian, O., Pogorielov, M. (2020). New Zr-Ti-Nb Alloy for Medical Application: Development, Chemical and Mechanical Properties, and Biocompatibility. Materials, 13 (6), 1306. https://doi.org/10.3390/ma13061306
7. Gnilitskyi, I., Pogorielov, M., Viter, R., Ferraria, A. M., Carapeto, A. P., Oleshko, O. et al. (2019). Cell and tissue response to nanotextured Ti6Al4V and Zr implants using high-speed femtosecond laser-induced periodic surface structures. Nanomedicine: Nanotechnology, Biology and Medicine, 21, 102036. https://doi.org/10.1016/j.nano.2019.102036
8. Ivasishin, O. M., Skiba, I. A., Karasevskaya, O. P., Markovskiy, P. E., Shivanyuk, V. N., Kalashnikov, A. V. et al. (2014). Fizicheskie principy sozdaniya nizkomodul'nyh splavov na osnove cirkoniya i titana dlya izgotovleniya implantatov. Litopys travmatolohiyi ta ortopediyi, 1-2 (29-30), 261.
9. Ivasyshyn, O. M., Skyba, I. O., Karasevska, O. P., Markovskyi, P. Ye. (2011). Pat. No. 102455 UA. Biocompatible alloy with low elasticity modulus containing zirconium and titanium (variants). No. a201115314; declareted: 26.12.2011; published: 10.07.2013, Bul. No. 13.
10. Mishchenko, O., Solodovnyk, O., Deineka, V., Oleshko, O. (2020). Cellular response (osteoblasts and fibroblasts) depending on the type of surface of dental implants. Morphologia, 14 (1), 42–49. https://doi.org/10.26641/1997-9665.2020.1.42-49
11. Frazier, W. E. (2014). Metal Additive Manufacturing: A Review. Journal of Materials Engineering and Performance, 23 (6), 1917–1928. https://doi.org/10.1007/s11665-014-0958-z
12. Gasser, A., Backes, G., Kelbassa, I., Weisheit, A., Wissenbach, K. (2010). Laser Additive Manufacturing. Laser Technik Journal, 7 (2), 58–63. https://doi.org/10.1002/latj.201090029
13. Azhazha, V. M., V'yugov, P. N., Lavrinenko, S. D., Lindt, K. A., Muhachev, A. P., Pipipenko, N. N. (1998). Cirkoniy i ego splavy: tekhnologi proizvodstva, oblast' primeneniya. Kharkiv: NN HFTI, 89.
14. Ovchynnykov, O. V., Khaznaferov, M. V. (2022). Vstup do adytyvnykh tekhnolohiy kolorovykh metaliv. Kyiv: Naukova dumka, 122.
15. Balachandramurthi, A. R., Moverare, J., Mahade, S., Pederson, R. (2018). Additive Manufacturing of Alloy 718 via Electron Beam Melting: Effect of Post-Treatment on the Microstructure and the Mechanical Properties. Materials, 12 (1), 68. https://doi.org/10.3390/ma12010068
16. Juechter, V., Scharowsky, T., Singer, R. F., Körner, C. (2014). Processing window and evaporation phenomena for Ti–6Al–4V produced by selective electron beam melting. Acta Materialia, 76, 252–258. https://doi.org/10.1016/j.actamat.2014.05.037
17. Ovchynnykov, O. V., Khaznaferov, M. V., Moisieiev, S. V., Mishchenko, O. M., Ovchynnykov, O. O. (2022). Pat. No. 128545 UA. A method for obtaining powder from spherical granules by plasma atomization of a workpiece and powder obtained by this method. No. a202200817; declareted: 22.02.2022; published: 08.08.2024, Bul. No. 34.
18. Hrabe, N., Quinn, T. (2013). Effects of processing on microstructure and mechanical properties of a titanium alloy (Ti–6Al–4V) fabricated using electron beam melting (EBM), Part 2: Energy input, orientation, and location. Materials Science and Engineering: A, 573, 271–277. https://doi.org/10.1016/j.msea.2013.02.065
19. Matviichuk, V. A., Nesterenkov, V. M., Berdnikova, O. M. (2022). Additive electron beam technology of manufacture of metal products from powder materials. Automatic Welding, 2, 16–25. https://doi.org/10.37434/as2022.02.03
20. Matviichuk, V. A., Nesterenkov, V. M. (2020). Additive electron beam equipment for layer-by-layer manufacture of metal products from powder materials. The Paton Welding Journal, 2020 (2), 41–46. https://doi.org/10.37434/tpwj2020.02.08
21. Matviichuk, V., Nesterenkov, V., Berdnikova, O. (2022). Determining the influence of technological parameters of the electron-beam surfacing process on quality indicators. Eastern-European Journal of Enterprise Technologies, 1 (12 (115)), 21–30. https://doi.org/10.15587/1729-4061.2022.253473
22. Matviichuk, V., Nesterenkov, V., Berdnikova, O. (2024). Determining the influence of technological parameters of electron beam surfacing process on the microstructure and microhardness of Ti-6Al-4V alloy. Eastern-European Journal of Enterprise Technologies, 1 (12 (127)), 6–12. https://doi.org/10.15587/1729-4061.2024.297773
23. Grade 23 Ti-6Al-4VELI Alloy (UNS R56401) (2013). AZOM. Available at: https://www.azom.com/article.aspx?ArticleID=9365
24. Bezymyanniy, Yu. G., Koziracкiy, E. A., Nazarenko, V. A., Teslenko, L. O. (2017). Osobennosti akusticheskih izmereniy v pressovkah na osnove poroshka titana. Visnyk NTU «KhPI», 4 (1226), 3–7.
25. Veretilnyk, O. V., Biktagirov, F. K. (2024). Electroslag processing of Kh18N10T stainless steel shavings. Electrometallurgy Today, 3, 31–35. https://doi.org/10.37434/sem2024.03.04
26. Zhai, Y., Galarraga, H., Lados, D. A. (2016). Microstructure, static properties, and fatigue crack growth mechanisms in Ti-6Al-4V fabricated by additive manufacturing: LENS and EBM. Engineering Failure Analysis, 69, 3–14. https://doi.org/10.1016/j.engfailanal.2016.05.036